Batrachotoxin-modified Sodium Channels in Planar Lipid Bilayers

Characterization of Saxitoxin- and Tetrodotoxin-induced Channel Closures

W. N. GREEN, L. B. WEISS, and O. S. ANDERSEN

From the Department of Physiology and Biophysics, Cornell University Medical College, New York 10021

ABSTRACT The guanidinium toxin–induced inhibition of the current through voltage-dependent sodium channels was examined for batrachotoxin-modified channels incorporated into planar lipid bilayers that carry no net charge. To ascertain whether a net negative charge exists in the vicinity of the toxin-binding site, we studied the channel closures induced by tetrodotoxin (TTX) and saxitoxin (STX) over a wide range of [Na^+]. These toxins carry charges of +1 and +2, respectively. The frequency and duration of the toxin-induced closures are voltage dependent. The voltage dependence was similar for STX and TTX, independent of [Na^+], which indicates that the binding site is located superficially at the extracellular surface of the sodium channel. The toxin dissociation constant, K_D, and the rate constant for the toxin-induced closures, k_c, varied as a function of [Na^+]. The Na^+ dependence was larger for STX than for TTX. Similarly, the addition of tetraethylammonium (TEA^+) or Zn^{++} increased K_D and decreased k_c more for STX than for TTX. These differential effects are interpreted to arise from changes in the electrostatic potential near the toxin-binding site. The charges giving rise to this potential must reside on the channel since the bilayers had no net charge. The Na^+ dependence of the ratios K_D^{STX}/K_D^{TTX} and k_c^{STX}/k_c^{TTX} was used to estimate an apparent charge density near the toxin-binding site of about $-0.33\ e\cdot nm^{-2}$. Zn^{++} causes a voltage-dependent block of the single-channel current, as if Zn^{++} bound at a site within the permeation path, thereby blocking Na^+ movement. There was no measurable interaction between Zn^{++} at its blocking site and STX or TTX at their binding site, which suggests that the toxin-binding site is separate from the channel entrance. The separation between the toxin-binding site and the Zn^{++} blocking site was estimated to be at least 1.5 nm. A model for toxin-induced channel closures is proposed, based on conformational changes in the channel subsequent to toxin binding.

Address reprint requests to Dr. Olaf S. Andersen, Dept. of Physiology and Biophysics, Cornell Medical College, 1300 York Ave., New York, NY 10021. Dr. Green's present address is Dept. of Physiology, Yale University School of Medicine, New Haven, CT 06510. Dr. Weiss's present address is Dept. of Anesthesiology, University Medical Center, Tucson, AZ 85724.

J. GEN. PHYSIOL. © The Rockefeller University Press · 0022-1295/87/06/0873/31 $1.00

Volume 89 June 1987 873–903

INTRODUCTION

The guanidinium toxins saxitoxin (STX) and tetrodotoxin (TTX) have played a critical role in the identification, characterization, and purification of voltage-dependent sodium channels (see reviews by Barchi, 1982; Agnew, 1984; Catterall, 1984). These toxins specifically and reversibly inhibit sodium channel currents (Narahashi et al., 1964; Hille, 1968), and appear to bind to a common extracellular site (Colquhoun et al., 1972; Wagner and Ulbricht, 1975). Although the molecular mechanism underlying the current inhibition is unknown, it has been proposed that it occurs when a toxin molecule binds and physically occludes the channel (Kao and Nishiyama, 1965; Hille, 1971, 1975; Kao and Walker, 1982). Despite the wide acceptance of this scheme, there is no direct experimental evidence supporting it.

Little is known about the structure and surface chemistry of the binding site, but comparative studies on STX- and TTX-induced closures indicate that there is a net negative charge near (or at) the binding site. At physiological pH, TTX has a charge of +1 (Woodward, 1964), while STX has a charge of +2 (Shimizu et al., 1981). The addition of Ca^{++} has a larger depressant effect on STX binding and current inhibition than on TTX binding and current inhibition (Henderson et al., 1974; Hille et al., 1975*a*), which indicates that Ca^{++} changed an electrostatic potential at the binding site. The reduction of toxin binding and current inhibition by protons suggests that the toxins bind to a group with an apparent pK_a of ~5.4 (Colquhoun et al., 1972; Ulbricht and Wagner, 1975*a*, *b*). Further, since toxin binding and current inhibition are removed by carboxylate-modifying reagents (Shrager and Profera, 1973; Baker and Rubinson, 1975; Reed and Raftery, 1976; Spalding, 1980), there is considerable evidence for a functionally important carboxylate group or groups at the toxin-binding site.

We have examined the STX- and TTX-induced channel closures of batrachotoxin (BTX)-modified Na channels incorporated into planar lipid bilayers to address three questions: Is there a net negative charge on the channel protein near the toxin-binding site? If so, how will this affect the kinetics of toxin binding and the interpretation of toxin-cation interactions at the binding site? What is the relation between the toxin-binding site and the permeation path? The various versions of the occlusion model place the toxin-binding site in or adjacent to the permeation path. The question of how the toxin molecule could close the channel can thus be addressed indirectly from information about the location of the toxin-binding site relative to the permeation path. We conclude that the toxin-binding site is distant from the permeation path, and propose a model for toxin-induced closures based on conformational changes in the channel. Preliminary reports of some of the work reported here have been presented elsewhere (Green et al., 1984*a–c*, 1986).

MATERIALS AND METHODS

Experimental Procedures and Materials

Voltage-dependent, BTX-modified sodium channels from canine forebrain were incorporated into planar lipid bilayers as described in the preceding article (Green et al., 1987).

All experiments were done at room temperature (22–25°C) at pH 7.4. Except where noted, the experiments were done with symmetrical solutions having Na^+ as the only cation and Cl^- as the major anion. In the text, the solutions are identified by their total Na^+ concentration and the concentration of the buffer (phosphate or HEPES). The makeup of the electrolyte solutions and other experimental procedures and materials were as described in Green et al. (1987). The orientation of the channels was established from their voltage-activation characteristics, and STX or TTX was added to the "extracellular" solution. Membrane potential differences are expressed relative to the extracellular solution.

Data Analysis

In the presence of the guanidinium toxins, BTX-modified sodium channels undergo spontaneous as well as toxin-induced closures that have very different average durations (cf. Figs. 1 and 2). Similar to what was found by French et al. (1984) and Moczydlowski et al. (1984*a*), little error is introduced if only closures lasting >600 ms are assigned to the toxin-induced category.

The toxin-induced closures were quantified as the fractional closed time, f_c:

$$f_c = \sum_{i=0}^{n} i \cdot T_c^i/(n \cdot T_{obs}), \tag{1}$$

where n is the total number of channels in the membrane, T_{obs} is the total observation time for the experiment, i is an index parameter ($0 \leq i \leq n$), and T_c^i is the total time i closed channels were observed, counting only closing events lasting >600 ms.

The average duration of the toxin-induced closures, τ_c, was estimated as:

$$\tau_c = f_c \cdot T_{obs}/n_t, \tag{2}$$

where n_t denotes the number of transitions accumulated during the time T_{obs}. The average time between toxin-induced closing events, τ_o, was estimated as:

$$\tau_o = (1 - f_c) \cdot T_{obs}/n_t. \tag{3}$$

Estimates of τ_c and τ_o were also obtained from dwell-time histograms, using a maximum-likelihood estimator (Hall and Sellinger, 1981). Statistical estimates of parameters in Eqs. 4, 5, 9, and 10 were obtained by fitting the equations to the data using a nonlinear least-squares fitting routine based on a combination of the grid search and Marquardt-Levenberg algorithms (e.g., Bevington, 1969, pp. 204–246), with inclusion of the "jackknife" procedure (e.g., R. G. Miller, 1974). Fits to Eqs. 11, 12, 14, or 15 together with Eq. 13 were done interactively.

RESULTS

Toxin-induced Closing Events

At membrane potentials positive to −60 mV, BTX-modified sodium channels are open most of the time in the absence of STX or TTX (see Fig. 1). Most spontaneous channel closures last <600 ms, and their closed-time distribution (Fig. 1*B*) cannot be described by a single-exponential decay, which indicates that there is more than one closed state of the channel (see also Moczydlowski et al., 1984*a*). In contrast, the open-time distribution (Fig. 1*C*) is reasonably well described by a single-exponential decay, which is consistent with a single open state.

The addition of nanomolar amounts of either STX or TTX to the extracellular solution resulted in very long-lived channel closures (Krueger et al., 1983; Green et al., 1984*c*; Moczydlowski et al., 1984*a*, *b*) (see Fig. 2*A*). (This figure depicts data obtained with TTX; similar results were obtained with STX.) The toxin-induced closures are complete; that is, the amplitude of the current transitions corresponds to the amplitude of the channels' unitary current steps (Green et al., 1987). The toxin action is reversible; it was abolished by perfusing the

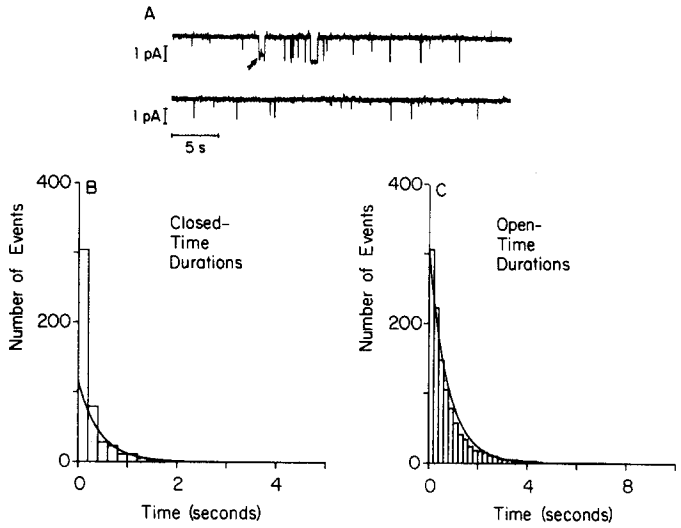

FIGURE 1. Spontaneous channel closures. The current traces in *A* illustrate spontaneous current transitions in a single BTX-modified sodium channel. The channel is open most of the time, but has occasional closing transitions to the fully closed state. The arrow points to a transition to a subconductance state. Experiment 850415: 0.5 M Na^+, 0.01 M HEPES, $\Delta V = +63$ mV, cutoff frequency = 40 Hz. (*B*) Survivor plot of spontaneous channel closures. The histogram is based on 304 transitions from a single channel. The subpopulation of channel closures that last >0.2 s were analyzed as a single-exponential decay: $N(t) = N \cdot \exp(-t/\tau)$, where $N(t)$ is the number of closed events of duration $\geq t$, N is the number of events in the population at $t = 0$, and τ is the mean closed time. There is an excess number of short-lived closures. $\tau = 0.42$ s, $N = 115$. Experiment 830810: 0.5 M Na^+, 0.01 M HEPES, $\Delta V = +60$ mV. (*C*) Survivor plot of the open-time distribution for the same channel. The distribution is described by a single-exponential decay. $N = 292$, $\tau = 0.78$ s.

extracellular solution with a toxin-free, but otherwise identical, solution (data not shown). Toxin-induced closures were not observed when the toxins were added to the intracellular solution. (Subconductance events [Green et al., 1987] may last substantially >600 ms. They are, however, easily recognized and cannot be mistaken for toxin-induced closures. There are no discernible differences between toxin binding to channels in the fully open state and that to channels in the subconductance or flickery states.)

The dwell-time histograms change after toxin addition, consistent with the appearance of a single population of long-lived closing events (Fig. 2, *B* and *C*). The frequency and mean duration of the short-lived closings are unaffected by the toxin addition (cf. Figs. 1 and 2); that is, the toxins induce a new type of closing event and have no effect on the frequency or duration of the events seen in the absence of toxin. The lifetime distribution of long-lived, toxin-induced channel closures can be described by a single-exponential decay (Fig. 2*B*). Similar

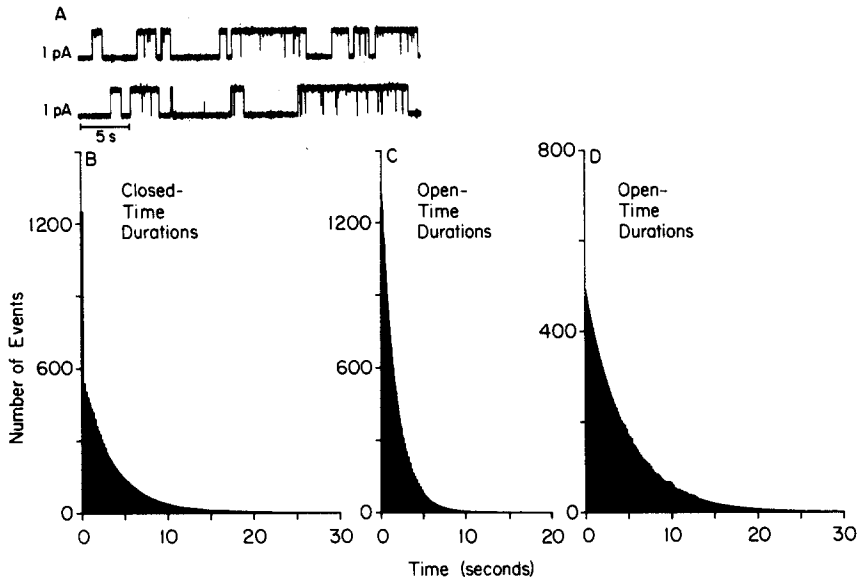

FIGURE 2. Toxin-induced channel closures. (*A*) Examples of TTX-induced closing events. Experiment 850415: 0.5 M Na^+, 0.01 M HEPES, ΔV = +63 mV, cutoff frequency = 140 Hz. (*B*) Survivor plot of spontaneous and TTX-induced channel closures. The histogram is based on 1,264 transitions from a single channel. The data for $t \geq 0.6$ s are described by a single-exponential decay. $N = 545$, $\tau = 3.6$ s. There is an excess number of brief channel closures. Experiment 850528: 0.5 M Na^+, 0.01 M HEPES, ΔV = 60 mV, 155 nM TTX. (*C*) Survivor plot of the open-time distribution for the same channel. The open-time distribution is described by a single-exponential decay. $N = 1324$, $\tau = 1.7$ s. (*D*) Survivor plot for 477 openings between closures lasting >0.6 s. The histogram is fitted by a single-exponential decay. $N = 488$, $\tau = 4.6$ s.

estimates for τ_c were obtained from a exponential fit to this subpopulation and from Eq. 2 (3.6 vs. 3.9 s).

The open-time distribution is also well described by a single-exponential decay (Fig. 2*C*). The interpretation of the data is complicated by the existence of several kinetically distinct closed states, and the time constant of the decay is not simply related to the rate of toxin binding. If the analysis is restricted to open times between closures lasting >600 ms, the distribution is also described by a single-exponential decay (Fig. 2*D*). The time constant of this distribution repre-

sents the mean time between toxin-induced channel closures and is related to the rate of toxin binding. Again, very similar estimates for τ_o were obtained from the exponential fit and from Eq. 3 (4.6 vs. 4.7 s). The single-exponential decay of the toxin-associated dwell-time distributions indicates that the toxins bind and produce reversible transitions between a single open and a single toxin-induced closed state.

Equilibrium Toxin Binding and Its Na^+ and Potential Dependence

The dose-response characteristics of toxin-induced channel closures can be quantified by the relation between the fractional closed time, f_c (Eq. 1), and [T], where T denotes the toxin, either STX or TTX. The data for STX and TTX in 0.05 M Na^+ are illustrated in Fig. 3. At high toxin concentrations, f_c approaches

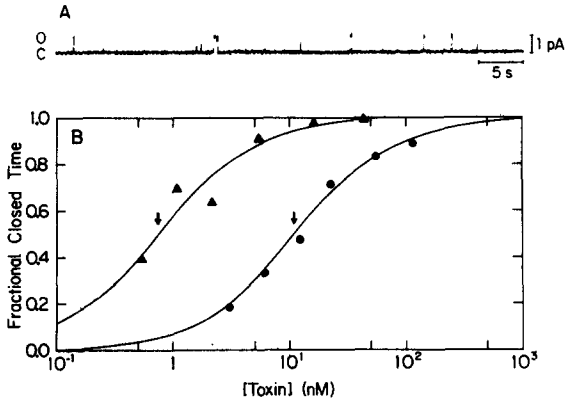

FIGURE 3. Dose-response curves for toxin block. (*A*) A two-channel current trace at high [STX]; both channels are closed most of the time. Occasional brief (upward) transitions to the open state are seen; f_c is very close to 1. [STX] is 60 times the magnitude of dissociation constant determined in *B*. Experiment 840706: 0.05 M Na^+, 0.01 M HEPES, 43.0 nM STX, ΔV = +60 mV. (*B*) f_c vs. toxin concentration for STX (▲) and for TTX (●). The curves denote the best fits of Eq. 4 to the data. For STX: $f_{c,max} = 1.01 \pm 0.03$, $K = 0.699 \pm 0.034$ nM; for TTX: $f_c = 1.01 \pm 0.03$, $K = 12.4 \pm 1.3$ nM. The arrows denote the K_D values. 0.05 M Na^+, 0.01 M HEPES, ΔV = 60 mV.

1. This saturation behavior is illustrated in Fig. 3*A*. Formally, the data can be described by a Langmuir isotherm:

$$f_c = f_{c,max} \cdot [T]/(K + [T]), \tag{4}$$

where $f_{c,max}$ is the maximum f_c, and K is the [T] at which $f_c = 0.5 \cdot f_{c,max}$. Because $f_{c,max}$ for both STX and TTX is indistinguishable from 1.0, binding-site occupancy and channel closure are indistinguishable within the limits set by the resolution. Therefore, f_c is interpreted to be the probability that the binding site is occupied by toxin, while K is interpreted to be the toxin's apparent dissociation constant, K_D. Given Eq. 4, and that $f_{c,max} \simeq 1.0$, K_D can be estimated based on a single determination of f_c at a given [T].

K_D for both STX and TTX varies as a function of the membrane potential difference, ΔV (French et al., 1984; Green et al., 1984*c*; Moczydlowski et al., 1984*a*, *b*) (see Fig. 4). The voltage dependence of $K_D(\Delta V)$ can be described by:

$$K_D(\Delta V) = K_D(0) \cdot \exp(\delta \cdot \Delta V \cdot e/kT), \quad (5)$$

where $K_D(0)$ is K_D at 0 mV, δ is an equivalent valence that quantifies how the applied potential affects toxin binding, e is the elementary charge, k is Boltzmann's constant, and T is the temperature in Kelvin. When Eq. 5 is fitted to the

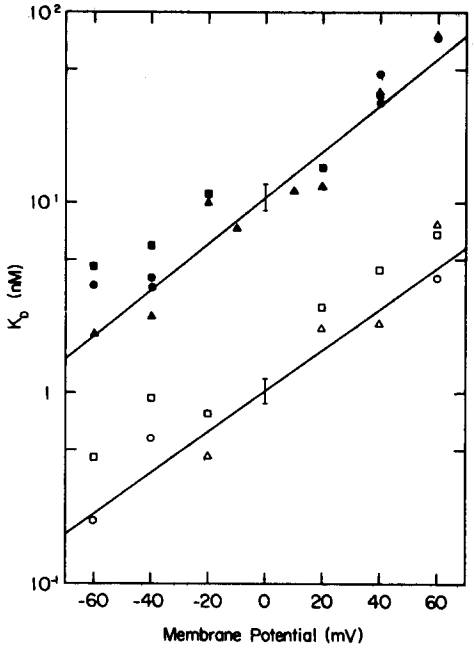

FIGURE 4. K_D as a function of ΔV for STX (open symbols) and TTX (filled symbols): (○) [STX] = 1.08 nM; (△) [STX] = 3.23 nM; (□) [STX] = 10.8 nM; (●) [TTX] = 6.1 nM; (▲) [TTX] = 18.3 nM; (■) [TTX] = 30.5 nM. (Most of the TTX data are from Green et al., 1984*c*, obtained with $[Na^+]$ = 0.116 M. In the data analysis, the $[Na^+]$ was set to 0.1 M.) The lines denote the best fits of Eq. 5 to the data (see text). The error bars at ΔV = 0 mV denote ±1 SD for $K_D(0)$. 0.1 M Na^+, 0.01 M HEPES or phosphate.

data in Fig. 4, the δ estimates are similar, 0.63 ± 0.08 for STX and 0.71 ± 0.10 for TTX. The $K_D(0)$ estimates differ 10-fold, however: 1.03 ± 0.15 nM for STX and 10.6 ± 1.6 nM for TTX.

The results from experiments at other $[Na^+]$ ($0.02 \leq [Na^+] \leq 3.5$ M) are summarized in Table I. The $K_D(0)$ values vary as functions of $[Na^+]$. The variation is more pronounced for the divalent STX than for the monovalent TTX. Estimates for δ vary by a factor of <2. At each $[Na^+]$, the difference between the δ estimates for STX and for TTX is within our experimental error. STX and TTX bind and close the channel with the same voltage dependence.

Kinetics of Toxin-induced Channel Closures

On the basis of the equilibrium experiments, the simplest kinetic scheme for the action of STX and TTX is that they induce transitions between two distinguishable channel states: an open, toxin-free state, O, and a closed, toxin-bound state, CT:

$$O + T \underset{k_o}{\overset{k_c}{\rightleftarrows}} CT, \qquad \text{(Scheme I)}$$

where k_c is the rate constant for toxin association with the channel and k_o is the rate constant for toxin dissociation from the channel. The rate constants are

TABLE I

Equilibrium Characteristics of STX- and TTX-induced Channel Closures

$[Na^+]$	n*	TTX, $K_D(0) \pm$ SD	$\delta \pm$ SD	n*	STX, $K_D(0) \pm$ SD	$\delta \pm$ SD	$K_D^{TTX}(0)/K_D^{STX}(0)$
M		*M*			*M*		
0.02	10	$2.5\pm0.3 \times 10^{-9}$	0.47±0.05	16	$6.3\pm0.2 \times 10^{-11}$	0.55±0.15	39.9
0.05	19	$3.0\pm0.8 \times 10^{-9}$	0.56±0.09	15	$1.6\pm0.1 \times 10^{-10}$	0.48±0.04	18.6
0.1	15	$1.1\pm0.2 \times 10^{-8}$	0.71±0.10	13	$1.0\pm0.1 \times 10^{-9}$	0.63±0.08	10.3
0.5	17	$3.5\pm0.5 \times 10^{-8}$	0.76±0.08	17	$8.3\pm3.2 \times 10^{-9}$	0.78±0.15	4.17
1.0	10	$5.1\pm2.3 \times 10^{-8}$	0.88±0.10	10	$3.5\pm0.8 \times 10^{-8}$	0.60±0.14	1.47
2.5	17	$2.5\pm0.6 \times 10^{-7}$	0.57±0.11	—	—	—	—
3.5	3	$3.6\pm2.3 \times 10^{-7}$	0.54±0.34	—	—	—	—

* n is the number of determinations for K_D ($-80 \le \Delta V \le +120$ mV).

related to the average duration of the toxin-induced open and closed times (e.g., Fig. 2):

$$k_c = 1/(\tau_o \cdot [T]), \qquad (6)$$

$$k_o = 1/\tau_c, \qquad (7)$$

and the toxin dissociation constant is:

$$K_D = k_o/k_c. \qquad (8)$$

Fig. 5 depicts open-time distributions at different [TTX]. These data, along with similar information for STX, and the associated closed-time data for both toxins are analyzed further in Fig. 6. Consistent with Scheme I, $1/\tau_o$ for STX and TTX increases in proportion to [T], while $1/\tau_c$ is almost independent of [T].

The voltage dependence of K_D results from voltage-dependent changes in both k_c and k_o. The rate constants for toxin-induced channel closures are plotted as a function of ΔV in Fig. 7. The voltage dependence of the rate constants can be expressed as

$$k_c(\Delta V) = k_c(0) \cdot \exp(-\delta_c \cdot \Delta V \cdot e/kT), \qquad (9)$$

and

$$k_o(\Delta V) = k_o(0) \cdot \exp(\delta_o \cdot \Delta V \cdot e/kT), \qquad (10)$$

where $k_c(0)$ and $k_o(0)$ denote the rate constants at 0 mV, and δ_c and δ_o are equivalent valences that quantify how the applied potential affects the corresponding rate constants. When Eqs. 9 and 10 are fitted to the data in Fig. 7, the estimates for k_o, δ_c, and δ_o are similar for STX and TTX, while the estimates for $k_c(0)$ differ 10-fold. The ratio $k_o(0)/k_c(0)$ is 1.41 nM for STX and 13.2 nM for TTX, and the sum $\delta_o + \delta_c$ is 0.58 and 0.63, in reasonable agreement with the K_D and δ estimates obtained from the f_c data.

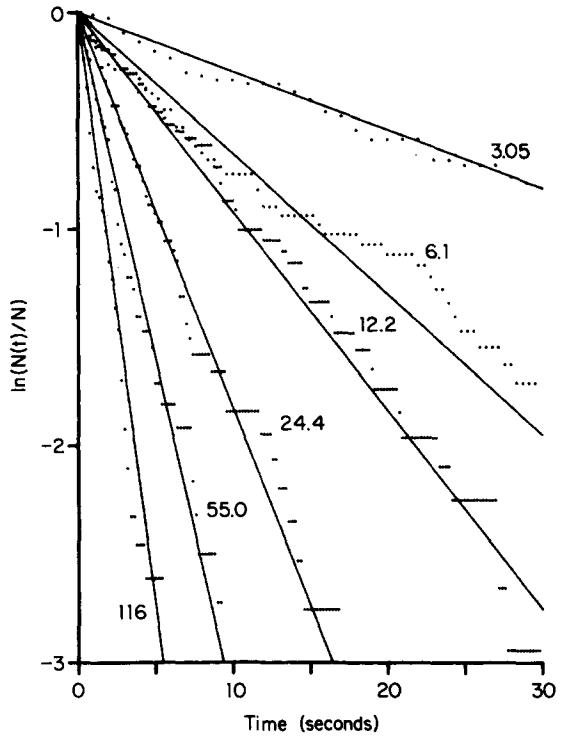

FIGURE 5. Open-time survivor plots as a function of [TTX]. The data are displayed as $\ln[N(t)/N]$ vs. t. Only openings occurring between closures ≥0.6 s were included in the distributions. The lines denote fits of single-exponential decays to the data. [TTX] = 3.05 nM: τ_o = 37.0 s and N = 79; for 6.1 nM: τ_o = 17.2 s and N = 61; for 12.2 nM: τ_o = 10.8 s and N = 57; for 24.4 nM: τ_o = 6.4 s and N = 63; for 51.0 nM: τ_o = 3.2 s and N = 61; and for 116 nM: τ_o = 1.9 s and N = 82. Experiment 831011: 0.05 M Na^+, 0.01 M HEPES, ΔV = 62 mV.

Experiments at other $[Na^+]$ ($0.02 \leq [Na^+] \leq 3.5$ M) are summarized in Table II. For both STX and TTX, $k_c(0)$ varies as function of $[Na^+]$. As for K_D, the variation is more pronounced for STX than for TTX. In contrast, the $k_o(0)$ estimates for STX and TTX vary little with changes in $[Na^+]$. The Na^+-dependent changes in K_D result primarily from changes in k_c. The δ_c estimates decrease slightly with decreasing $[Na^+]$, while those for δ_o vary little with $[Na^+]$. Interestingly, there are consistent differences between the δ_c and δ_o estimates for

the toxins, the δ_c estimates for STX being larger than for TTX, with the opposite pattern for the δ_o estimates.

The Na^+ dependence of the k_o estimates does not arise from a bias in our data-reduction procedures. Similar behavior is observed when the closed-time distributions are analyzed as a function of $[Na^+]$ at a constant ΔV (Fig. 8). For each of the three Na^+ concentrations, the data are well described by a single-exponential decay; there is no evidence for the existence of two distinct closed states among

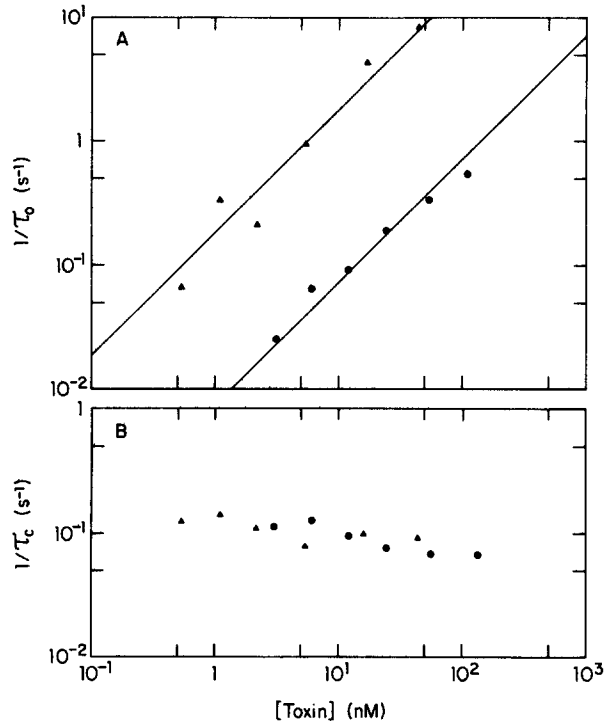

FIGURE 6. Toxin concentration dependence of channel closing and opening rates. (*A*) Plot of $1/\tau_o$ vs. toxin concentration for STX (▲) and TTX (●). The data are from the same records used to determine the f_c values in Fig. 3. The lines are drawn with a slope of 1.0. (*B*) Plot of $1/\tau_c$ vs. toxin concentration for the experiments shown in *A*.

the long-lived channel closures. The same (Na^+-dependent) variation is observed in the $k_o(+60)$ values as in the $k_o(0)$ estimates.

Is There a Negative Electrostatic Potential at the Toxin-binding Site?

It has been proposed that there is a negative electrostatic potential (relative to the bulk solution) at the toxin-binding site (Henderson et al., 1974; Hille et al., 1975*a*). Such a potential difference, arising from negative charges at or close to the toxin-binding site, could explain why K_D, or k_c, estimates for STX vary as a stronger function of $[Na^+]$ than the corresponding estimates for TTX (Green

and Andersen, 1986). Increases in [Na^+] could change toxin binding by competitively displacing the toxins as well as by changing the potential at the binding site by screening the fixed negative charges. Such a screening will change the local [T] (and [Na^+]), and the [T] changes will be larger for STX, which carry a charge of +2, than for TTX, which carry a charge of +1.

An extension of the two-state model (Scheme I) to include competitive interactions between Na^+ and toxin and fixed charges in the vicinity of the toxin-

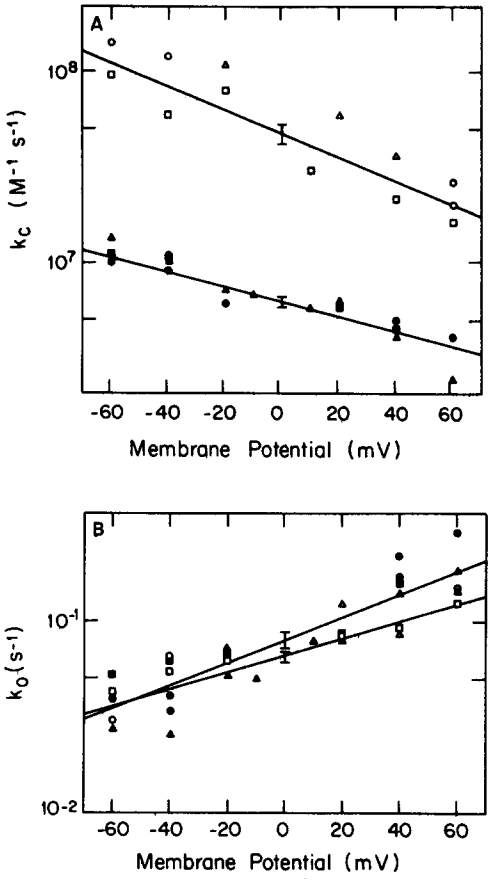

FIGURE 7. k_c and k_o as a function of ΔV for STX (open symbols) and TTX (filled symbols). The symbols denote the toxin concentrations indicated in Fig. 3. (*A*) k_c; (*B*) k_o. The rate constants are calculated using Eqs. 1–3 and 6–7 from the records used to estimate the K_D values in Fig. 3. The lines denote fits of Eqs. 9 and 10 to the data. For STX: $k_c(0) = 4.7 \pm 0.5 \times 10^7$ $M^{-1} \cdot s^{-1}$, $\delta_c = 0.37 \pm 0.03$, $k_o(0) = 6.6 \pm 0.5 \times 10^{-2}$ s^{-1}, and $\delta_o = 0.26 \pm 0.05$. For TTX: $k_c(0) = 6.1 \pm 0.3 \times 10^6$ $M^{-1} \cdot s^{-1}$, $\delta_c = 0.23 \pm 0.03$, $k_o(0) = 8.1 \pm 0.7 \times 10^{-2}$ s^{-1}, and $\delta_o = 0.35 \pm 0.07$. The error bars at $\Delta V = 0$ mV denote ±1 SD for $k_c(0)$ and $k_o(0)$. 0.1 M Na^+, 0.01 M HEPES or phosphate.

TABLE II

Kinetic Characteristics of STX- and TTX-induced Channel Closures

[Na^+]	Toxin	n*	$k_c(0) \pm$ SD	$\delta_c \pm$ SD	$k_o(0)$	$\delta_o \pm$ SD
M			$M^{-1} \cdot s^{-1}$		s^{-1}	
0.02	TTX	10	$2.2 \pm 0.1 \times 10^7$	0.15±0.03	$5.8 \pm 0.6 \times 10^{-2}$	0.32±0.07
0.02	STX	16	$5.3 \pm 0.5 \times 10^8$	0.28±0.06	$5.1 \pm 0.3 \times 10^{-2}$	0.29±0.03
0.05	TTX	19	$1.3 \pm 0.1 \times 10^7$	0.24±0.04	$4.7 \pm 0.5 \times 10^{-2}$	0.26±0.05
0.05	STX	15	$3.1 \pm 0.5 \times 10^8$	0.33±0.06	$6.6 \pm 0.4 \times 10^{-2}$	0.19±0.03
0.1	TTX	15	$6.1 \pm 0.3 \times 10^6$	0.23±0.03	$8.1 \pm 0.7 \times 10^{-2}$	0.35±0.07
0.1	STX	13	$4.7 \pm 0.5 \times 10^7$	0.37±0.05	$6.6 \pm 0.5 \times 10^{-2}$	0.26±0.05
0.5	TTX	17	$1.5 \pm 0.2 \times 10^6$	0.24±0.05	$7.1 \pm 0.8 \times 10^{-2}$	0.44±0.04
0.5	STX	17	$4.4 \pm 1.3 \times 10^6$	0.36±0.14	$8.6 \pm 0.5 \times 10^{-2}$	0.32±0.04
1.0	TTX	10	$1.2 \pm 0.1 \times 10^6$	0.37±0.06	$5.8 \pm 0.9 \times 10^{-2}$	0.48±0.14
1.0	STX	10	$2.1 \pm 0.2 \times 10^6$	0.52±0.07	$8.9 \pm 0.8 \times 10^{-2}$	0.21±0.07
2.5	TTX	17	$4.3 \pm 0.4 \times 10^5$	0.26±0.03	$1.7 \pm 1.0 \times 10^{-1}$	0.28±0.02
3.5	TTX	3	$3.2 \pm 0.5 \times 10^5$	0.40±0.08	$1.2 \pm 0.8 \times 10^{-1}$	0.1±0.3

* n is the number of determinations for k_c and k_o ($-80 \leq \Delta V \leq +120$ mV).

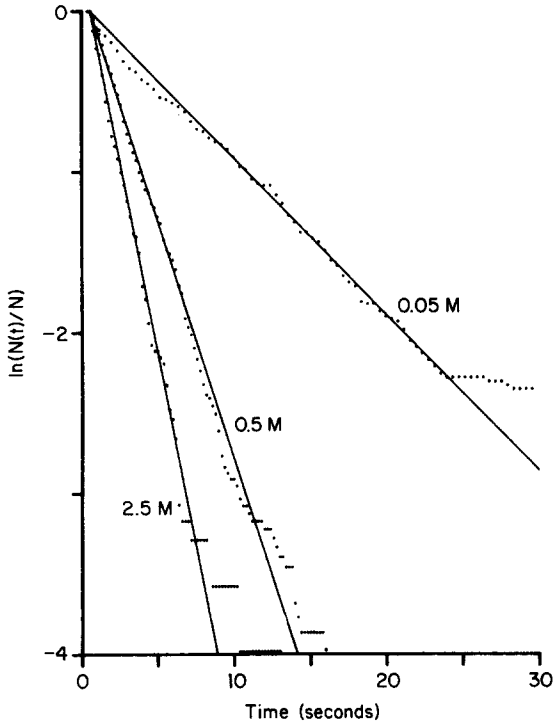

FIGURE 8. Closed-time survivor plots for TTX at three different [Na^+]. The data are displayed as $\ln[N(t)/N]$ vs. t. Only channel closures lasting >0.6 s were included in the distributions. The lines denote fits of single-exponential decays to the data. For 0.05 Na^+ M (rightmost data set): $\tau_c = 11.4$ s and $N = 411$ ($n = 419$); for 0.5 Na^+ M (middle data set): $\tau_c = 3.6$ s and $N = 545$ ($n = 478$); for 2.5 Na^+ M (leftmost data set): $\tau_c = 2.7$ s and $N = 226$ ($n = 214$). Experiment 831011: 0.05 M Na^+, 0.01 M HEPES, $\Delta V = 62$ mV; experiment 840528: 0.5 M Na^+, 0.01 M HEPES, $\Delta V = 60$ mV; experiment 831122: 2.5 M Na^+, 0.01 M phosphate, $\Delta V = 56$ mV.

binding site is developed in the Discussion and the Appendix. According to the extended model, K_D (or k_c) for STX and TTX will vary as functions of both [Na^+] and the electrostatic potential at the binding site, V_s (see Eqs. 14 and 15). The (competitive) Na^+ dependence, however, will not appear in the ratio K_D^{STX}/K_D^{TTX}:

$$K_D^{STX}([Na^+], V_s)/K_D^{TTX}([Na^+], V_s) = (K_D^{STX}/K_D^{TTX})\cdot\exp(V_s\cdot e/kT), \quad (11)$$

or the ratio k_c^{STX}/k_c^{TTX}:

$$k_c^{STX}([Na^+], V_s)/k_c^{TTX}([Na^+], V_s) = (\kappa_c^{STX}/\kappa_c^{TTX})\cdot\exp(-V_s\cdot e/kT), \quad (12)$$

where the K_D values on the right-hand side of Eq. 11 denote the toxin dissociation constants when V_s and [Na^+] are both zero, and the κ_c values on the right-hand side of Eq. 12 denote the corresponding association rate constants. The relation between the charge distribution, [Na^+], and V_s is not known. As a first approximation, the Gouy-Chapman equation will be used (e.g., Aveyard and Haydon, 1973):

$$V_s = (2\cdot kT/e)\cdot\text{arcsinh}\{\sigma/(8\cdot[Na^+]\cdot\epsilon_o\cdot\epsilon_r\cdot kT)^{0.5}\}, \quad (13)$$

where σ is an apparent charge density at the binding site, ϵ_o is the permittivity of free space, and ϵ_r is the relative dielectric constant of water (78.5 at 24°C as estimated from Weast, 1972, p. E-49). (The presence of divalent $HPO_4^=$ was ignored; this will not affect the estimates for V_s.) The K_D and k_c ratios are plotted as functions of [Na^+] in Fig. 9. The solid curves were drawn according to Eqs. 11 or 12 and 13 with $\sigma = -0.33\ e\cdot nm^{-2}$, $K_D^{STX}/K_D^{TTX} = 1.0$, and $k_c^{STX}/k_c^{TTX} = 0.8$. The estimates for K_D^{STX}/K_D^{TTX} and σ can vary, because the parameters are correlated. An almost equally good fit was obtained when $K_D^{STX}/K_D^{TTX} = 1.5$ and $\sigma = -0.4\ e\cdot nm^{-2}$. Acceptable fits are obtained when the parameter set varies between these limits. (In Fig. 9*B*, we also plotted k_o^{STX}/k_o^{TTX} as a function of [Na^+], to emphasize that the differential effect of [Na^+] changes on STX and TTX results from changes in the local [T] and that the Na^+ dependence of k_o is the same for both toxins.)

Since Eqs. 12 and 13 can describe the [Na^+] dependence of the K_D ratios, there may be a negative potential (and a net negative charge) in the vicinity of the toxin-binding site. The next two sections report results of experiments designed to explore this point further.

Effects of Monovalent Cations on Toxin-induced Channel Closures

If there is a net negative charge near the toxin-binding site, the addition of "inert" electrolytes to the extracellular aqueous phase will produce differential decreases in the apparent affinity for TTX and STX. (Ideally, an inert Na^+ substitute should not be permeant through the channel; neither should it block the channel, compete with toxins at their binding site, or bind to the channel, thereby altering the net charge. It is not clear that any truly inert cations exist, and some of the ions used here interact with the sodium channel. This should not, however, affect our main conclusions.) The ionic strength was increased using the Cl^- salts of tetraethylammonium (TEA^+) and *N*-methylglucamine (NMG^+). Increases in ionic strength using TEA^+ decreased the STX affinity

more than the TTX affinity, without affecting the voltage dependence of the channel closures. A decrease in the STX affinity was also observed when the ionic strength was increased with NMG^+. The data for k_c, k_o, and K_D are summarized in Table III.

Importantly, the decreases in K_D were caused by decreases in k_c, whereas the k_o values were unaffected by these maneuvers. The k_c changes were related to ionic strength changes in the extracellular phase. (The small increases in k_o for TTX and k_c for STX with 0.02 M TEA^+ in the intracellular phase are within the uncertainties in our estimates of the rate constants.) The larger decreases in STX affinity, relative to the TTX affinity changes, are consistent with the existence of a net negative charge near the toxin-binding site (see also Table VI and the related text of the Discussion).

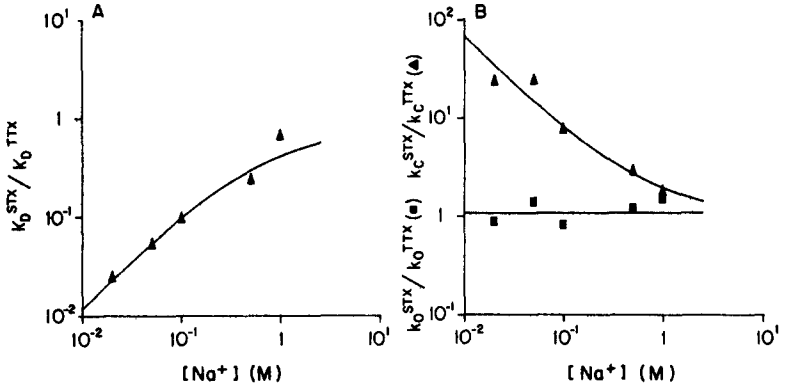

FIGURE 9. Differential effects of $[Na^+]$ on STX- and TTX-induced channel closures. (*A*) $K_D^{STX}([Na^+])/K_D^{TTX}([Na^+])$ vs. $[Na^+]$. The curve denotes a fit of Eqs. 11 and 13 to the data (see text). (*B*) (▲) $k_c^{STX}([Na^+])/k_c^{TTX}([Na^+])$ vs. $[Na^+]$; (■) $k_o^{STX}([Na^+])/k_o^{TTX}([Na^+])$ vs. $[Na^+]$. The curved line denotes a fit of Eqs. 12 and 13 to the k_c data (see text). The straight line is drawn to emphasize that there is no systematic trend in the k_o data.

Effects of Divalent Cations on Toxin-induced Channel Closures

Divalent cations screen fixed negative charges better than monovalent cations (e.g., McLaughlin, 1977). The effects of two divalent cations, Ba^{++} and Zn^{++}, were examined to further test for screening of fixed negative charges and to evaluate the relation between the permeation path and the toxin-binding site.

The addition of 0.005 M Ba^{++} to an extracellular solution containing 0.02 M Na^+ results in a fourfold increase in K_D for STX (Table IV). The effects of Ba^{++} were similar to the effects of TEA^+ and NMG^+, except that Ba^{++} was effective at lower concentrations.

Zn^{++} had a much larger effect than Ba^{++}. When 0.0008 M $Zn(NO_3)_2$ was added to an extracellular solution containing 0.02 M Na^+, K_D for STX and TTX increased 10-fold and 2-fold, respectively (Table IV). Again, the changes in K_D

TABLE III

Effects of Monovalent Cations on Toxin-induced Channel Closures

$[Na^+]$	n*	M^+	$[M^+]$	Toxin	$K_D(0) \pm SD$	$\delta \pm SD$	$k_c(0) \pm SD$	$\delta_c \pm SD$	$k_o(0) \pm SD$	$\delta_o \pm SD$
M			*M*		*M*		$M \cdot s^{-1}$		s^{-1}	
0.02	5	TEA^+	0.08	TTX	$3.7 \pm 0.8 \times 10^{-9}$	0.50±0.14	$1.3 \pm 0.2 \times 10^{7}$	0.11±0.08	$5.5 \pm 0.6 \times 10^{-2}$	0.35±0.07
0.02	6	TEA^+	0.08	STX	$1.0 \pm 0.4 \times 10^{-9}$	0.54±0.24	$2.2 \pm 1.1 \times 10^{7}$	0.2±0.3	$5.2 \pm 0.5 \times 10^{-2}$	0.31±0.11
0.05	4	TEA^+	0.05	STX	$6.0 \pm 1.2 \times 10^{-10}$	0.55±0.10	$1.4 \pm 0.2 \times 10^{8}$	0.32±0.10	$6.4 \pm 3.6 \times 10^{-2}$	0.2±0.3
0.05	9	TEA^+	0.02‡	TTX	$4.6 \pm 0.3 \times 10^{-9}$	0.41±0.05	$1.3 \pm 0.1 \times 10^{7}$	0.18±0.05	$6.9 \pm 0.7 \times 10^{-2}$	0.24±0.02
0.05	4	TEA^+	0.02‡	STX	$5.3 \pm 0.7 \times 10^{-10}$	0.50±0.08	$1.3 \pm 0.3 \times 10^{8}$	0.20±0.11	$7.3 \pm 0.8 \times 10^{-2}$	0.29±0.06
0.05	5	NMG^+	0.15	STX	$2.3 \pm 0.5 \times 10^{-9}$	0.56±0.15	$1.6 \pm 0.4 \times 10^{7}$	0.28±0.12	$4.5 \pm 0.5 \times 10^{-2}$	0.29±0.06

Except for the values marked with asterisks, the inert electrolytes were added to both aqueous phases.

* n is the number of determinations of K_D, k_c, and k_o ($-60 \leq \Delta V \leq +60$ mV).

‡ Added to the intracellular solution only.

TABLE IV

Effects of Divalent Cations on Toxin-induced Channel Closures

$[Na^+]$	n*	D^{++}	$[D^{++}]$	Toxin	$K_D(0) \pm SD$	$\delta \pm SD$	$k_c(0) \pm SD$	$\delta_c \pm SD$	$k_o(0) \pm SD$	$\delta_o \pm SD$
M			*M*		*M*		$M \cdot s^{-1}$		s^{-1}	
0.02	8	Ba^{++}	0.005	STX	$2.6 \pm 0.3 \times 10^{-10}$	0.38±0.20	$1.2 \pm 0.1 \times 10^{8}$	0.14±0.06	$3.1 \pm 0.5 \times 10^{-2}$	0.24±0.08
0.02	5	Zn^{++}	0.0008	TTX	$3.7 \pm 1.3 \times 10^{-9}$	0.64±0.15	$1.2 \pm 0.3 \times 10^{7}$	0.14±0.16	$5.3 \pm 1.2 \times 10^{-2}$	0.59±0.13
0.02	14	Zn^{++}	0.0008	STX	$9.8 \pm 0.5 \times 10^{-10}$	0.46±0.03	$3.9 \pm 0.2 \times 10^{7}$	0.14±0.03	$3.9 \pm 0.4 \times 10^{-2}$	0.34±0.05

Zn^{++} was added to the extracellular side only. Ba^{++} was added to both aqueous phases. In one of eight determinations for STX, it was added to the extracellular side only.

* n is the number of determinations of K_D, k_c, and k_o ($-60 \leq \Delta V \leq +60$ mV).

resulted from changes in k_c, while there was little effect on k_o or the voltage dependences.

The finding that Zn^{++} has little effect on the voltage dependence of K_D (or of k_c and K_o) is important, because Zn^{++} causes a voltage-dependent (fast) block of

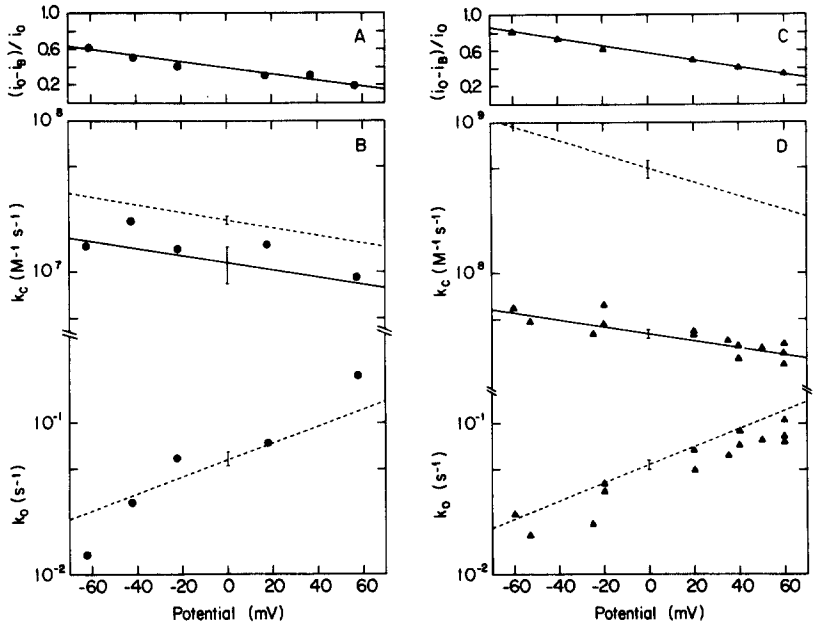

FIGURE 10. The effect of extracellular Zn^{++} on $k_c(\Delta V)$ and $k_o(\Delta V)$. (*A* and *B*) Data for TTX. (*A*) The fractional occupancy of Zn^{++} at its blocking site, $(i_o - i_B)/i_o$, as a function of ΔV (see Green et al., 1987), where i_o is the unblocked current and i_B is the current in the presence of Zn^{++}. The line through the points was drawn by eye. Experiment 841120: 0.02 M Na^+, 0.0008 M Zn^{++} was added to the extracellular solution, 0.005 M HEPES. (*B*) k_c and k_o as a function of ΔV with 0.0008 M Zn^{++} in the extracellular solution. The solid line denotes a fit of Eqs. 9 and 10 to the k_c data (see Table IV). The dashed lines denote fits of Eqs. 9 and 10 to k_c and k_o for TTX without Zn^{++} (see Table II). The error bars at $\Delta V = 0$ mV denote ±1 SD for $k_c(0)$ and $k_o(0)$. (*C* and *D*) Data for STX. (*C*) The fractional occupancy of Zn^{++} as a function of ΔV. The line through the points was drawn by eye. Experiment 841025: 0.02 M Na^+, 0.0008 M Zn^{++} was added to the extracellular solution, 0.005 M HEPES. (*D*) k_c and k_o as a function of ΔV with 0.0008 M Zn^{++} in the extracellular solution. The solid line denotes a fit of Eqs. 9 and 10 to the k_c data (see Table IV). The dashed lines denote fits of Eqs. 9 and 10 to k_c and k_o for TTX without Zn^{++} (see Table II). The error bars at $\Delta V = 0$ mV denote ±1 SD for $k_c(0)$ and $k_o(0)$.

the current through voltage-dependent sodium channels (Green et al., 1987). The characteristics of this block are consistent with Zn^{++} entering and binding some point down-field from the channel entrance (see Green et al., 1987, for details). If the toxin-binding site is close to the site where Zn^{++} binds, there will be electrostatic (repulsive) interactions between Zn^{++} and toxin. These interac-

tions will be more pronounced as the membrane is hyperpolarized, since the fractional occupancy for Zn^{++} at its blocking site will increase as ΔV becomes more negative. Any interaction between Zn^{++} and toxin should alter the voltage dependence of the toxin-induced channel closures. No pronounced effect on the voltage dependence was observed (Fig. 10). In Fig. 10, *A* and *C*, the fractional occupancy of Zn^{++} is plotted as a function of membrane potential. The k_c and k_o estimates for TTX and STX are plotted in *B* and *D*, respectively. For TTX, the addition of Zn^{++} decreased k_c twofold at all potentials, while k_o was unaffected. Electrostatic interactions between toxin and Zn^{++}, at their respective binding sites, will be larger for STX and Zn^{++} than for TTX and Zn^{++}. For STX, there was an ~10-fold decrease in k_c, with little effect on k_o. δ_c was decreased, but no more than in the Ba^{++} experiments, and δ_o was unaffected. There appears to be no electrostatic interactions between a Zn^{++} at its blocking site and a toxin molecule at its binding site.

DISCUSSION

One Toxin Molecule Closes One Channel

It is generally assumed that STX and TTX bind to a common site and that channel closure results from the binding of one toxin molecule to one channel (Hille, 1968; Colquhoun et al., 1972; Schwarz et al., 1973). This assumption implies a particular channel structure: a single lumen that connects the extracellular and intracellular aqueous phases. However, many channels exhibit multiple conductance states, and recent structural studies on *Escherichia coli* porin channels suggest that a channel may have three separate entrances at one side of a membrane that merge into one large outlet on the other side (Engel et al., 1985). If each entrance could be closed independently, the relation between membrane conductance and toxin concentration would be described by Eq. 4, which is suggestive of all-or-none closures, but an examination of the single-channel closures would show toxin-induced transitions to intermediate conductance levels. This is not observed in native (Quandt et al., 1985) or BTX-modified sodium channels (e.g., Krueger et al., 1983; Green et al., 1984*c*; Moczydlowski et al., 1984*a*, *b*; see also Fig. 2 in this article). The toxins close the channels in an all-or-none fashion. Further, the shape of the dose-response curves for single-channel closures (Figs. 3 and 6) strongly suggests that a channel is closed by one toxin molecule. The data therefore provide no support for cooperative interactions between two toxin molecules (e.g., Benoit and Dubois, 1985) in closing BTX-modified sodium channels. (Channel closures could depend on the binding of two toxin molecules, if the two toxin molecules bind with different affinities. If the second molecule binds with an affinity that is at least 10-fold less than the first, the dose-response curve would approximate a simple Langmuir binding isotherm. Therefore, if the BTX modification disrupted a positively cooperative toxin binding, our data would be consistent with the proposal of Benoit and Dubois [1985]. This model, however, is difficult to reconcile with the lack of interactions between BTX and STX in equilibrium binding studies [Catterall et al., 1979; Krueger et al., 1979; but see Brown, 1986].)

Evidence for Fixed Negative Charges in the Vicinity of the Binding Site

Monovalent cations inhibit toxin binding by a one-to-one competition between cation and toxin (Henderson et al., 1973; Reed and Raftery, 1976; Weigele and Barchi, 1978; Barchi and Weigele, 1979). If simple competition were the sole mechanism for cation-toxin interactions, changes in the (monovalent or divalent) cation concentration should alter the apparent affinities for STX and TTX to the same extent. Contrary to this prediction, increases in $[Ca^{++}]$ decrease the binding and current inhibition by STX more than the binding and inhibition by TTX (Henderson et al., 1974; Hille et al., 1975*a*). The magnitude of the differential effect on the monovalent and divalent toxins can be accounted for by screening of a net negative fixed charge (Ritchie and Rogart, 1977). Consistent with this interpretation, the addition of $[La^{+++}]$ produces similar differential effects on the STX- and TTX-induced current inhibition as are produced by much larger concentrations of divalent cations (Grissmer, 1984).

Rhoden and Goldin (1979) found that the Na^+ inhibition of STX binding to rat brain sodium channels exhibited a higher-order dependence than would be predicted by a one-to-one competitive interaction between Na^+ and toxin. This "cooperative" effect of monovalent cations on the STX affinity could result if there were a net negative charge in the vicinity of the binding site, since the ionic strength was not maintained constant in these experiments. When the ionic strength is maintained constant, $[Na^+]$ changes do not alter V_s and the interaction between STX and Na^+ is well described as a one-to-one competition (Weigele and Barchi, 1978; Barchi and Weigele, 1979).

There are thus compelling reasons to conclude that extracellular electrolytes affect toxin binding and channel closure through both competitive interactions with the toxins and screening of fixed charges. This conclusion is confirmed and extended by our findings. Our data strongly support the existence of a net negative charge in the vicinity of the guanidinium toxin–binding site. Similar to previous studies, various cations, i.e., Na^+, TEA^+, and Zn^{++}, alter STX-induced closures to a greater extent than TTX-induced closures, from which we conclude that there is a net charge in the vicinity of the toxin-binding site. Moreover, since the experiments were done using bilayers that carry no net charge, the charge (or charges) that influences cation and toxin interactions with the binding site must be on the sodium channel protein itself. (We do not know whether these charges originate in the protein proper or in the associated carbohydrate moiety. Indirect evidence suggests that part of the functionally significant negative charge may reside in the carbohydrate. As $[Na^+]$ decreases, the channel-to-channel scatter of the STX k_c values increases and becomes significantly larger than that of the TTX k_c values [e.g., Fig. 7]. These variations could result from channel microheterogeneities, similar to those observed on sodium dodecyl sulfate polyacrylamide gels, which presumably arise from channel-to-channel variations in glycosylation [Barchi, 1983; J. A. Miller et al., 1983].)

Independent support for this conclusion is provided by studies on BTX-modified rat muscle sodium channels, where k_c for STX derivatives that carry net charges between −1 and +2 varies systematically with the net charge, which suggests that in 0.2 M NaCl, the binding site is ~40 mV negative relative to the

aqueous phase (Moczydlowski et al., 1986). Models for the interactions between toxins and cations at the toxin-binding site should therefore incorporate specific competitive binding of cations to the toxin-binding site and screening of a net negative charge. (It may also be necessary to consider nonspecific ion binding, which would alter the charge distribution in the vicinity of the binding site.) A simple model, incorporating one-to-one competition between toxin and monovalent cations (e.g., $[Na^+]$) and screening of fixed charges in the vicinity of the toxin-binding site, is developed in the Appendix. The $[Na^+]$ and V_s dependence of K_D and k_c for STX and TTX can be expressed as:

$$K_D([Na^+], V_s) = K_D \cdot \exp(V_s \cdot z \cdot e/kT) \cdot \{1 + [Na^+] \cdot \exp(-V_s \cdot e/kT)/K_{Na}\} \quad (14)$$

and

$$k_c([Na^+], V_s) = \kappa_c \cdot \exp(-V_s \cdot z \cdot e/kT)/\{1 + [Na^+] \cdot \exp(-V_s \cdot e/kT)/K_{Na}\}, \quad (15)$$

where z is the valence of the toxin (+1 for TTX, +2 for STX), K_{Na} is the dissociation for Na^+ at the toxin-binding site, and K_D and κ_c denote the values of K_D and k_c in the absence of competing ions and without an electrostatic potential at the binding site ($V_s = 0$ mV).

In Fig. 11*A*, $k_c(0)$ for STX and TTX (from Table II) is plotted as a function of $[Na^+]$. As in Fig. 9, the charge distribution in the vicinity of the toxin-binding site is approximated by a uniformly smeared charge density, σ, and the relation between V_s, σ, and $[Na^+]$ was approximated by the Gouy-Chapman equation (Eq. 13). This combined competion and screening model (Eqs. 13 and 15) provides a good description of the Na^+ dependence of both the STX and TTX data. The solid curves in Fig. 11*A* were calculated using the same value of σ as in Fig. 9, $-0.33\ e \cdot nm^{-2}$, with $\kappa_c^{STX} = \kappa_c^{TTX} = 3 \times 10^6\ M^{-1} \cdot s^{-1}$, and $K_{Na} = 0.3$ M.

The difference in the Na^+ dependence for the STX and TTX data in Fig. 11*A* cannot be explained by a simple one-to-one competitive interaction between Na^+ and toxin, where the Na^+ dependence of $k_c(0)$ is given by:

$$k_c(0) = \kappa_c(0)/(1 + [Na^+]/K_{Na}), \quad (16)$$

where $\kappa_c(0)$ is the toxin's association rate constant in the absence of competing ions (at $[Na^+] = 0$). For $[Na^+] \geq K_{Na}$, $\log k_c(0)$ should decrease as an approximately linear function of $\log [Na^+]$, with a slope whose magnitude is <1. For the TTX data, the slope is about −0.85, while the STX data scatter around a line with a slope of −1.6 (Green and Andersen, 1986). The STX data therefore cannot be fitted by the simple competitive model (Eq. 16). The $\kappa_c(0)$ and K_{Na} estimates obtained by fitting Eq. 16 to the TTX data are displayed in Table V. These estimates differ by one order of magnitude from those derived from a fit of the combined competition and screening model (Eqs. 13 and 15) to the data.

For a simple (Gouy-Chapman) screening of fixed charges, the Na^+ dependence of $k_c(0)$ is given by:

$$k_c(0) = \kappa_c(0) \cdot \exp(-V_s \cdot z \cdot e/kT), \quad (17)$$

where V_s is a function of $[Na^+]$ (e.g., Eq. 13). In Fig. 11*B*, $k_c(0)$ is plotted as a function of V_s (calculated from Eq. 13 with $\sigma = -0.33\ e \cdot nm^{-2}$). The data for

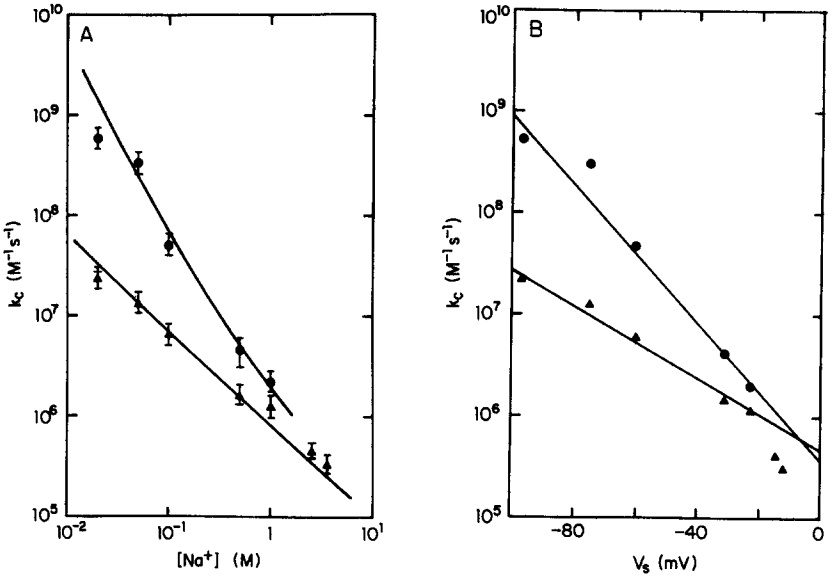

FIGURE 11. [Na^+] dependence of k_c for STX and TTX. (*A*) $k_c(0)$ for STX (▲) and TTX (●) as a function of [Na^+]. The curves denote fits of Eqs. 13 and 15 to the data (see text). (*B*) $k_c(0)$ for STX (▲) and TTX (●) as functions of V_s. The plot is a transform of *A* where V_s was determined from Eq. 13 (with $\sigma = -1/300$ $e \cdot Å^{-2}$). The lines denote linear regressions to the data for [Na^+] ≤ 1.0 M. The slopes were -0.018 mV^{-1} for STX and -0.034 mV^{-1} for TTX (which should be compared with the theoretical expectations: -0.017 and -0.034 mV^{-1}, respectively); $\kappa_c(0)$ was 4×10^5 $M^{-1} \cdot s^{-1}$ for STX and 5×10^5 $M^{-1} \cdot s^{-1}$ for TTX.

both STX and TTX are well described by the simple screening model (Eqs. 13 and 17) for $V_s < -20$ mV (or [Na^+] ≤ 1.0 M); $\kappa_c(0)$ estimates obtained from a fit of Eqs. 13 and 17 to the data are listed in Table V. They are one order of magnitude smaller than the estimates obtained when including Na^+-toxin competition in the model. At high [Na^+] (≥2.5 M), there are deviations from predictions based on the simple screening model, as would be expected from Na^+-toxin competitive interactions. The deviations could also result because the approximations and assumptions underlying our use of the Gouy-Chapman theory break down at high ionic strengths.

TABLE V

Comparison of Parameters for Toxin-induced Channel Closures

Model	$\kappa_c(0)$	K_{Na}	σ
	$M^{-1} \cdot s^{-1}$	M	$e \cdot nm^{-2}$
Simple competition (Eq. 16)*	3×10^7	3×10^{-2}	—
Simple screening (Eqs. 13 and 17)	5×10^5	—	−0.33‡
Competition and screening (Eqs. 13 and 15)	3×10^6	3×10^{-1}	−0.33‡

* Based on a fit to the TTX data only (Green and Andersen, 1986).

‡ Based on the fit in Fig. 9.

At a constant [Na^+], the addition of TEA^+ or Zn^{++} decreased the efficacy of the toxin to induce channel closures. The decreases were larger for the STX-induced than for the TTX-induced channel closures. If the only action of the inert cations were to affect V_s through screening of fixed negative charges as described by Gouy-Chapman theory, the changes in $k_c(0)$ should be predicted from Eqs. 13 and 15. These predictions, and predictions based on the simple screening model (Eqs. 13 and 17), are summarized in Table VI and compared with the measured values. There is good qualitative agreement between the predicted and measured rate constants, but neither the simple screening model nor the combined competition and screening model is clearly superior over the other. The argument for competitive interactions between Na^+ and toxin de-

TABLE VI

Observed vs. Predicted Effects of Cations on Toxin-induced Channel Closures

					$k_c(0)$		
						Predicted	
[Na^+]	C	[C]	T	V_s	Observed	Competition and screening*	Screening only‡
M		M		mV		$M^{-1}\cdot s^{-1}$	
0.02	—	—	TTX	−97	2.2×10^7	3.3×10^7	2.2×10^7
0.02	TEA^+	0.08	TTX	−59	1.3×10^7	1.8×10^7	5.1×10^6
0.02	Zn^{++}	0.0008	TTX	−80§	1.2×10^7	2.7×10^7	1.1×10^7
0.02	—	—	STX	−97	5.3×10^8	1.5×10^9	7.5×10^8
0.02	TEA^+	0.08	STX	−59	2.2×10^7	1.9×10^8	4.1×10^7
0.02	Zn^{++}	0.0008	STX	−80§	3.9×10^7	6.0×10^8	2.0×10^8
0.02	Ba^{++}	0.005	STX	−62§	1.2×10^8	2.2×10^8	5.1×10^7
0.05	—	—	STX	−75	3.1×10^8	2.5×10^8	1.4×10^8
0.05	TEA^+	0.05	STX	−59	1.4×10^8	1.2×10^8	4.1×10^7
0.05	NMG^+	0.15	STX	−46	1.6×10^7	5.4×10^7	1.4×10^7

* Predicted values based on the model combining screening of fixed charges and competitive interactions between toxin and Na^+ (i.e., Eqs. 13 and 15).

‡ Predicted values based on the screening model (i.e., Eqs. 13 and 17).

§ Calculated using an extension of Eq. 13, for mixed monovalent and divalent electrolytes (e.g., Aveyard and Haydon, 1973, Eq. 2.29).

pends on the equilibrium binding data at a constant ionic strength (*vide supra*). Our inability to distinguish between these models results, in part, because the local [Na^+] according to the predictions of the Gouy-Chapman theory of the diffuse double layer approaches a lower limit, $\sigma^2/(2\cdot\epsilon_o\cdot\epsilon_r\cdot kT)$ as the bulk [Na^+] $\rightarrow$ 0 (e.g., McLaughlin et al., 1971). (This limit is ~0.8 M for $\sigma = -0.33$ $e\cdot nm^{-2}$.) The changes in V_s will thus produce 5-fold changes in the local [Na^+], while the local [T] changes will be 4- and 16-fold for TTX and STX, respectively. For TTX, the changes in the local [Na^+] and [T] almost cancel in their effect on toxin binding; for STX, most of the affinity changes result from the V_s-dependent changes in the local [T].

Since Zn^{++} decreases $k_c(0)$ more than Ba^{++}, the effect of Zn^{++} cannot be explained solely by screening of fixed negative charges. Furthermore, if we

calculate V_s assuming a constant σ ($-0.33\ e\cdot nm^{-2}$), neither the simple screening (Eqs. 13 and 17) nor the combined competition and screening model (Eqs. 13 and Eq. 15) accurately predict the changes in $k_c(0)$. The deviations were larger for STX than for TTX. It appears that TEA^+ and Zn^{++} reduce V_s more than can be accounted for by their screening action, which suggests that TEA^+ and Zn^{++} reduce the net charge by binding in the vicinity of the toxin-binding site. Specific binding of Zn^{++} to sodium channels has been postulated to explain the effects of extracellular Zn^{++} on the channels' voltage activation (Hille et al., 1975*b*) and gating charge movement (Gilly and Armstrong, 1982).

Discrepancies between predicted and observed effects may also arise because the charge distribution in the vicinity of the toxin-binding site was approximated by a uniformly smeared charge density. This approximation works well for the lipid bilayer/electrolyte interface (McLaughlin, 1977; Winiski et al., 1986), but may fail when used to describe ligand binding to proteins where only a few (relatively immobile) charged residues are likely to be important. (The cross-sectional areas of STX and TTX are ~0.5 nm^2. If the cross-sectional area of the toxin-binding site is similar and involves a carboxyl group with a pK of ~5.5, as suggested by titration studies [Colquhoun et al., 1972; Ulbricht and Wagner, 1975*a*, *b*] and covalent modification experiments [Sigworth and Spalding, 1980; Spalding, 1980], this single charge could be the major contributor to the apparent charge density of $-0.33\ e\cdot nm^{-2}$.)

Additionally, STX is not a point charge; it has two guanidinium groups separated by ~0.4 nm (as estimated from CPK models). This complication should not be serious, however, because dimethonium $[(CH_3)_3N^+(CH_2)_2N^+(CH_3)_3]$, which has a separation between the charged groups similar to that for STX, behaves as a classic (point charge) divalent cation at the lipid bilayer/electrolyte interface (McLaughlin et al., 1983). Finally, K_D varies as a function of the electrostatic field in the protein. At a constant ΔV, changes in the electrostatic potential at the extracellular surface of the protein will alter the field in the protein. This field variation could affect the equilibrium and kinetic aspects of toxin binding over and above what would be expected from the isolated change in V_s at the toxin-binding site. It would not, however, affect estimates based on the ratios of STX and TTX equilibrium or rate constants (Fig. 9).

The Location of the Toxin-binding Site

STX and TTX could close voltage-dependent sodium channels by several mechanisms: they could bind and physically occlude the channel (entrance); they could bind at a distant site and exert their effect on ion movement through electrostatic interactions with the permeating ions; or they could close the channel through a conformational change. On the basis of circumstantial evidence, it is widely assumed that the toxins physically occlude the channel by binding at its extracellular entrance (e.g., Catterall, 1980; Hille, 1984), but the other alternatives remain viable (e.g., Mullins, 1973; Hille, 1984, p. 302).

At a first glance, the voltage dependence of the toxin-induced channel closures supports a model in which the toxins enter and block the channel. In this case, the voltage dependence of closing would reflect the electrical distance between the extracellular aqueous phase and the binding site times the toxin valence

(Woodhull, 1973). However, the results of previous studies (Krueger et al., 1983; Green et al., 1984*c*; Moczydlowski et al., 1984*a*, *b*) and of this study are at odds with this interpretation. The similarity of the δ estimates for STX and TTX over a wide range of $[Na^+]$ provides additional evidence that only a small fraction (<0.1) of an applied potential difference falls between the bulk extracellular solution and the toxin-binding site (Green et al., 1984*c*; Moczydlowski et al., 1984*b*). The binding site must be quite superficial at the extracellular surface of the channel. The voltage dependence therefore results from voltage-dependent changes in the channel (Green et al., 1984*c*; Moczydlowski et al., 1984*b*): transitions between high- and low-affinity states (Moczydlowski et al., 1984*b*) or conformational changes leading to channel closure subsequent to toxin binding (see the next section).[1]

The question remains whether the toxin-binding site is "close to" (e.g., partially covering) or "far from" (spatially separate) the permeation path. We addressed this question indirectly, by studying the effect of the intracellular and extracellular impermeant ions TEA^+ and Zn^{++} on the toxin-induced channel closures. TEA^+ exerts a voltage-dependent block at the intracellular channel entrance (Green et al., 1987); ~0.5 of the applied potential appears to fall between the intracellular solution and the TEA^+-blocking site. There were no measurable interactions between a STX or TTX molecule at their binding site and a TEA cation that blocks from the intracellular solution (Table III). The lack of a TEA^+ effect argues that the TEA^+-blocking site and the toxin-binding site are too far apart to have significant electrostatic interactions between cations at these sites.

A similar argument could be made with respect to the position of the toxin-binding site relative to the Zn^{++}-blocking site. Zn^{++} exerts a voltage-dependent block at the extracellular channel entrance (Green et al., 1987); ~0.2 of the applied potential appears to fall between the extracellular solution and the Zn^{++}-blocking site. The addition of Zn^{++} to the extracellular solution decreased k_c for STX, while k_c for TTX was hardly affected. In neither case were there apparent effects on k_o (Table IV).

It is possible to estimate the interaction energy, ΔG_{int}, between Zn^{++} at its blocking site and STX at its binding site, from the changes in STX binding in the absence and presence of Zn^{++} and the changes in Zn^{++} occupancy at its blocking site, Δf_{Zn}. In the absence of Zn^{++}, the standard free energy for STX binding at an applied potential, ΔV, is

$$\Delta G°(\Delta V) = kT \cdot \ln[K_D(\Delta V)] = \Delta G°(0) + \delta \cdot e \cdot \Delta V, \quad (18)$$

where $\Delta G°(0)$ is the standard free energy at $\Delta V = 0$. The difference in binding energy at $\pm\Delta V$ is

$$\Delta\Delta G°(\Delta V) = \Delta G°(+\Delta V) - \Delta G°(-\Delta V) = kT \cdot \ln[K(+\Delta V)/K(-\Delta V)], \quad (19)$$

[1] Experiments on the node of Ranvier show no evidence for a voltage-dependent TTX inhibition of current flow through native, chloramine T–, or veratridine-modified sodium channels (Rando and Strichartz, 1985, 1986). The voltage dependence of the toxin-induced channel closures is a result of the BTX modification. Note, however, that the voltage dependence of the current inhibition, irrespective of its origin, provides an additional tool for studying voltage-dependent sodium channels.

which can be simplified as

$$\Delta\Delta G^{\circ}(\Delta V) = 2 \cdot \delta \cdot e \cdot \Delta V. \tag{20}$$

In the presence of Zn^{++}, one similarly finds that

$$\Delta\Delta G(\Delta V)_{Zn} = 2 \cdot \delta_{Zn} \cdot e \cdot \Delta V + \Delta f_{Zn}(\Delta V) \cdot \Delta G_{int}, \tag{21}$$

where δ_{Zn} is the voltage dependence of $K_D(\Delta V)$ in the presence of Zn^{++}. If there are no interactions between Zn^{++} and STX in the aqueous phase,

$$\Delta G_{int} = 2 \cdot (\delta - \delta_{Zn}) \cdot e \cdot \Delta V / \Delta f_{Zn}(\Delta V). \tag{22}$$

For $\Delta V = 60$ mV, $\Delta f_{Zn}(60)$ is ~0.6, while $(\delta - \delta_{Zn}) = 0.11 \pm 0.15$ (cf. Tables II and IV). We thus estimate ΔG_{int} to be 22 ± 30 meV, and a reasonable upper limit on ΔG_{int} is 2 kT. If the interactions between the bound Zn^{++} and STX are predominantly electrostatic (through the protein):

$$\Delta G_{int} \simeq (2 \cdot e)^2 / (4 \cdot \pi \cdot \epsilon_o \cdot \epsilon_r \cdot d_{1,2}), \tag{23}$$

where $d_{1,2}$ is the distance between the sites, and ϵ_r is an average dielectric constant. For ΔG_{int} to be $\leq 2\ kT$, the $\epsilon_r \cdot d_{1,2}$ product must be $\geq 1.1\ 10^2$ nm. ϵ_r is between 3 and 80 (Pethig, 1979; Honig et al., 1986), and $d_{1,2}$ is estimated to be >1.5 nm. (A slightly larger minimum separation is obtained if the interactions predominantly result from changes in V_s, owing to changes in Zn^{++} binding, in which case the minimum separation should be comparable to the Debye length in 0.02 M monovalent salt, ~2 nm.)

The large separation between the Zn^{++}-blocking site and the toxin-binding site could occur if the permeation path is long (~10 nm) and fairly narrow, such that it can be occupied simultaneously by Zn^{++} (or TEA^+) and a toxin molecule with no electrostatic interaction between the two blocking ions. Alternatively, the toxin-binding site is spatially distinct, and distant from the permeation path. The available information supports a structure where the permeation path and the toxin-binding site are distinct. In covalent modification experiments, the single-channel conductance can be modified with no apparent effect on toxin binding (Chabala et al., 1986).[2] Similar experiments on sodium channels in the frog node of Ranvier show that carboxyl groups at the extracellular channel entrance seem to be distinct from those in the vicinity of the toxin-binding site (Gülden and Vogel, 1985). Similarly, it appears that the apparent charge density at the binding site can differ from that at the extracellular channel entrance (Neumcke and Stämpfli, 1986). The lack of electrostatic interactions between toxins at their binding site and ions in the permeation path further implies that the toxins cannot close the channel by physically occluding the permeation path or through electrostatic interactions with the permeating ions. The most likely

[2] Worley et al. (1986) concluded that the toxin-binding site is at the extracellular channel entrance. This conclusion was based on the complete identity between trimethyloxonium-induced modifications of toxin binding and of single-channel conductance under conditions expected to lead to an almost complete modification of carboxylate groups. An alternative interpretation is that modification of a carboxylate group in the binding site leads to a conformational change in the channel, thereby decreasing the conductance.

mechanism for the toxin-induced closures of voltage-dependent sodium channels is a conformational change that closes the channel.

A Model for Toxin-induced Channel Closure

On the basis of the preceding discussion, models for guanidinium toxin–induced closure of BTX-modified sodium channels should incorporate two features: the voltage dependence of the toxin-induced closures should arise from voltage-dependent changes in the channel protein, and the channel closure should result through conformational changes that occur subsequent to toxin binding. A minimal model incorporating these features is obtained by extending Scheme I to include an intermediary (third) state, where the toxins are bound to a sodium channel in the conducting state. A channel in this state can then undergo a voltage-dependent conformational change to close the channel:

$$\mathrm{O} + \mathrm{T} \underset{k_{-1}}{\overset{k_1}{\rightleftharpoons}} \mathrm{OT} \underset{\beta(\Delta V)}{\overset{\alpha(\Delta V)}{\rightleftharpoons}} \mathrm{CT}. \qquad \text{(Scheme II)}$$

In this scheme, O is a conducting state with no toxin at its binding site, OT is a conducting state with a toxin at its binding site, and CT is the nonconducting state with a toxin at its binding site. For simplicity, the voltage dependence of the inhibition is assigned to the rate constants for transitions between OT and CT, $\alpha(\Delta V)$, and $\beta(\Delta V)$. This model differs from that proposed by Moczydlowski et al. (1984*b*) in that channel closure is not associated with toxin binding per se, but to conformational changes that occur subsequent to toxin binding. Scheme II can be extended to incorporate a voltage-dependent binding reaction, O + T $\rightleftarrows$ OT, by introducing additional voltage-dependent equilibria between two O and between two OT states, as was done by Moczydlowski et al. (In any case, the voltage dependence of the toxin-induced channel closures appears to be an incidental finding, a consequence of the BTX modification [Rando and Strichartz, 1985, 1986]. The important point for native channels is that the channel closures in Scheme II occur subsequent to toxin binding.)

Solving the kinetic equations corresponding to Scheme II, the dose-response curve is

$$f_c = \gamma \cdot [\mathrm{T}]/\{K_1 + (\gamma + 1) \cdot [\mathrm{T}]\}, \qquad (24)$$

where $K_1 = k_{-1}/k_1$, and $\gamma(\Delta V) = \alpha(\Delta V)/\beta(\Delta V)$. Comparing Eq. 4 with Eq. 24,

$$f_{c,\max} = \gamma/(\gamma + 1), \qquad (25)$$

and

$$K_D = K_1/(\gamma + 1). \qquad (26)$$

Experimentally, f_c approaches 1 as $[\mathrm{T}] \to \infty$ (Fig. 3). Therefore, $\gamma/(\gamma + 1) \simeq 1$, $\gamma \gg 1$, and $K_D \simeq K_1/\gamma$ in the potential range investigated here. In this model, the high toxin affinity results from the conformational change(s) that occurs subsequent to the initial binding, not from the binding reaction(s) per se.

According to Scheme II, survivor plots of toxin-induced closed times should be described by single-exponential decays, as was observed (Figs. 2 and 8). This

implies that

$$k_o = \beta. \tag{27}$$

[If α is not much less than k_{-1}, there may be several OT $\rightleftarrows$ CT transitions during the time a toxin molecule is bound to the channel. If these transitions cannot be resolved, $\tau_c^{-1} \simeq \beta \cdot k_{-1}/(\alpha + k_{-1})$.]

According to Scheme II, survivor plots of the intervals between toxin-induced channel closures should generally be described as the sum of two-exponential decays. But only a single-exponential decay was observed (Figs. 2 and 5), which implies that

$$k_c = \alpha/K_1. \tag{28}$$

[Generally, $1/(\tau_o \cdot [T]) \simeq \alpha \cdot k_1/(\alpha + k_{-1} + k_1 \cdot [T])$. For k_c to be independent of [T], $k_1 \cdot [T] \ll \alpha + k_{-1}$; further, if $\alpha \ll k_{-1}$, Eq. 28 is obtained.]

Toxin action depends on a protonated guanidinium group (C_7—C_8—C_9 in STX [Hille, 1968], and C_1—C_2—C_3 in TTX) and several hydroxyl groups (the C_{12} gem diol in STX and the C_9 and C_{10} hydroxyls in TTX [Kao and Walker, 1982; Strichartz, 1984; Kao and Yasumoto, 1985]). The existence of two classes of functional groups on the toxin molecules suggests in itself a two-step reaction for toxin-induced channel closures, similar to Scheme II. The hydroxyl groups on the toxin may be involved in the initial binding reaction, O $\rightarrow$ OT, since the removal of functionally important hydroxyl groups decreases binding affinity without abolishing toxin action. The conformational change that closes the channel may involve interactions between the functionally important guanidinium groups and carboxyl groups at the toxin-binding site, since toxin action is completely abolished by modifying sodium channels with carboxyl group–specific reagents (Shrager and Profera, 1973; Baker and Rubinson, 1975; Reed and Raftery, 1976; Spalding, 1980).

The conformational change(s) could cause a positive entity (e.g., an arginyl or a lysyl residue) to move into the channel lumen to abolish ion movement. Some support for this hypothesis is provided by the observation that the toxin-Na^+ interactions are not classically competitive, as k_o increased with increasing [Na^+] (Fig. 8). There thus seem to be (weak) interactions between a toxin at its binding site and Na^+ interacting with the channel at some other site. A similar observation was made by Ulbricht and Wagner (1975*b*) in studies on toxin-H^+ interactions, where the rate constant for relief of current inhibition increased when the extracellular [H^+] was increased.

Our conclusion that the toxin-binding site is distant from the channel entrance raises the question, why is the toxin-binding site so highly conserved through evolution? One would expect parts of the channel not essential for function to be more susceptible to evolutionary pressures, and less likely to be conserved, than functionally significant parts. Since TTX-sensitive sodium channels are found in phyla ranging from *Annelida* to *Chordata* (e.g., Hille, 1984, p. 374), it appears that the toxin-binding site is essential for channel function, but is not involved in ion movement through the open permeation path. Possible functional roles are that the toxin-binding site is involved in channel gating, e.g., inactivation, or slow inactivation (the voltage dependence of K_D appears when slow

inactivation is inhibited [Rando and Strichartz, 1985]); that the toxin may bind at a site that is critical for subunit or domain interactions in the channel; or that the toxins mimic endogenous ligands that bind to the receptor.

APPENDIX

Competitive Toxin-Na^+ Interactions at a Charged Binding Site

Let, O, CT, and ONa^+ denote channel states where the toxin-binding site is unoccupied (by toxin or Na^+), occupied by toxin (T), and occupied by Na^+. The competitive interaction between T and Na^+ is described by:

$$O + T \underset{k_o}{\overset{\kappa_c}{\rightleftarrows}} CT, \qquad \text{(Scheme AI)}$$

and

$$O + Na^+ \underset{k_{-Na}}{\overset{k_{Na}}{\rightleftarrows}} ONa^+, \qquad \text{(Scheme AII)}$$

subject to the constraint that $W(O) + W(CT) + W(ONa^+) = 1$, where W denotes the probability of finding the channel in the three states.

Solving the kinetic equations corresponding to Schemes AI and AII,

$$K_D = K_D \cdot (1 + [Na^+]/K_{Na}), \qquad \text{(A1)}$$

where $K_D = k_o/\kappa_c$ and $K_{Na} = k_{Na}/k_{-Na}$, and the concentrations (and the rate constants and dissociation constants) refer to the local concentrations at the toxin-binding site.

The local [T] and $[Na^+]$ will differ from their bulk concentrations, $[T]_b$ and $[Na^+]_b$, when the electrostatic potential at the binding site differs from that of the bulk solution. If the average time the binding site is unoccupied is long compared with the electric and diffusive relaxation times of the diffuse part of the double layer adjacent to the binding site, the local concentrations can be related to the bulk concentrations by the Boltzmann equation:

$$[T] = [T]_b \cdot \exp(-V_s \cdot z \cdot e/kT), \qquad \text{(A2)}$$

and

$$[Na^+] = [Na^+]_b \cdot \exp(-V_s \cdot e/kT), \qquad \text{(A3)}$$

where V_s denotes the potential difference between the binding site and the bulk solution (when the binding site is vacant), and z is the toxin valence.

When related to the bulk aqueous concentration, the rate constant for toxin association with the binding site, k_c, becomes:

$$k_c = \kappa_c \cdot \exp(-V_s \cdot z \cdot e/kT)/\{1 + [Na^+]_b \cdot \exp(-V_s \cdot e/kT)/K_{Na}\}. \qquad \text{(A4)}$$

For a simple competitive interaction, k_o should not be affected by changes in $[Na^+]$, and the desired expression for K_D, as related to the bulk aqueous concentrations is

$$K_D = K_D \cdot \exp(V_s \cdot z \cdot e/kT) \cdot \{1 + [Na^+]_b \cdot \exp(-V_s \cdot e/kT)/K_{Na}\}. \qquad \text{(A5)}$$

We thank J. W. Daly, National Institutes of Health, for the generous gift of batrachotoxin. We also thank L. D. Chabala, D. B. Cherbavaz, and E. Recio-Pinto for assistance with some of the experiments, L. D. Chabala and B. W. Urban for helpful discussions, and D. B. Cherbavaz for the artwork.

This work was supported by grant GM-21342 and training grant AM-07152 from the National Institutes of Health, and by the Departmental Associates Program at Cornell University Medical College.

Original version received 15 July 1986 and accepted version received 16 February 1987.

REFERENCES

Agnew, W. S. 1984. Voltage-regulated sodium channel molecules. *Annual Review of Physiology.* 46:517–530.

Aveyard, R., and D. A. Haydon. 1973. An Introduction to the Principles of Surface Chemistry. Cambridge University Press, London. 232 pp.

Baker, P. F., and K. A. Rubinson. 1975. Chemical modification of crab nerves can make them insensitive to the local anaesthetics tetrodotoxin and saxitoxin. *Nature.* 257:412–414.

Barchi, R. L. 1982. Biochemical studies of the excitable membrane sodium channel. *International Review of Neurobiology.* 23:69–101.

Barchi, R. L. 1983. Protein components of the purified sodium channel from rat skeletal muscle sarcolemma. *Journal of Neurochemistry.* 40:1377–1385.

Barchi, R. L., and J. B. Weigele. 1979. Characteristics of saxitoxin binding to the sodium channel of sarcolemma isolated from rat skeletal muscle. *Journal of Physiology.* 295:383–396.

Benoit, E., and J.-M. Dubois. 1985. Cooperativity of tetrodotoxin in the frog node of Ranvier. *Pflügers Archiv.* 405:237–243.

Bevington, P. R. 1969. Data Reduction and Error Analysis for the Physical Sciences. McGraw-Hill, New York. 336 pp.

Brown, G. B. 1986. ^{3}H-batrachotoxin-A benzoate binding to voltage-sensitive sodium channels: inhibition by the channel blockers tetrodotoxin and saxitoxin. *Journal of Neuroscience.* 6:2064–2070.

Catterall, W. A. 1980. Neurotoxins that act on voltage-sensitive sodium channels in excitable membranes. *Annual Review of Toxicology.* 20:15–43.

Catterall, W. A. 1984. The molecular basis of neuronal excitability. *Science.* 223:653–661.

Catterall, W. A., C. S. Morrow, and R. P. Hartshorne. 1979. Neurotoxin binding to receptor sites associated with voltage-sensitive sodium channels in intact, lysed, and detergent-solubilized brain membranes. *Journal of Biological Chemistry.* 254:11379–11387.

Chabala, L. D., W. N. Green, O. S. Andersen, and C. L. Borders, Jr. 1986. Covalent modification of external carboxyl groups of batrachotoxin-modified canine forebrain sodium channels. *Biophysical Journal.* 49:40*a*. (Abstr.)

Colquhoun, D., R. Henderson, and J. M. Ritchie. 1972. The binding of labelled tetrodotoxin to non-myelinated nerve membranes. *Journal of Physiology.* 227:95–126.

Engel, A., A. Massalski, H. Schindler, D. L. Dorset, and J. P. Rosenbusch. 1985. Porin channel triplets merge into single outlets in *Escherichia coli* outer membranes. *Nature.* 317:643–645.

French, R. J., J. F. Worley, and B. K. Krueger. 1984. Voltage-dependent block by saxitoxin of sodium channels incorporated into lipid bilayers. *Biophysical Journal.* 45:301–310.

Gilly, W. F., and C. M. Armstrong. 1982. Slowing of sodium channel opening kinetics in squid axon by extracellular zinc. *Journal of General Physiology.* 79:935–964.

Green, W. N., and O. S. Andersen. 1986. Surface charge near the guanidinium neurotoxin binding site. *Annals of the New York Academy of Sciences.* 479:306–312.

Green, W. N., L. B. Weiss, and O. S. Andersen. 1984*a*. Voltage- and Na^+-dependent tetrodotoxin (TTX) block of batrachotoxin (BTX)-modified sodium channels. *Biophysical Journal.* 45:68*a*. (Abstr.)

Green, W. N., L. B. Weiss, and O. S. Andersen. 1984*b*. Gating and tetrodotoxin (TTX) block of batrachotoxin (BTX)-modified sodium channels in bilayers. *8th International Biophysics Congress*. 8:275. (Abstr.)

Green, W. N., L. B. Weiss, and O. S. Andersen. 1984*c*. Batrachotoxin-modified sodium channels in lipid bilayers. *Annals of the New York Academy of Sciences*. 435:548–550.

Green, W. N., L. B. Weiss, and O. S. Andersen. 1986. The tetrodotoxin and saxitoxin binding site of voltage-dependent sodium channels in negatively charged and distant from the permeation pathway. *Biophysical Journal*. 49:40*a*. (Abstr.)

Green, W. N., L. B. Weiss, and O. S. Andersen. 1987. Batrachotoxin-modified sodium channels in planar lipid bilayers. Ion permeation and block. *Journal of General Physiology*. 89:841–872.

Grissmer, S. 1984. Effect of various cations and anions on the action of tetrodotoxin and saxitoxin on frog myelinated nerve fibers. *Pflügers Archiv*. 402:352–359.

Gülden, K.-M., and W. Vogel. 1985. Three functions of sodium channels in the toad node of Ranvier are altered by trimethyloxonium ions. *Pflügers Archiv*. 403:13–20.

Hall, P., and B. Sellinger. 1981. Better estimates of exponential decay parameters. *Journal of Physical Chemistry*. 85:2941–2946.

Henderson, R., J. M. Ritchie, and G. R. Strichartz. 1973. The binding of labelled saxitoxin to the sodium channels in nerve membrane. *Journal of Physiology*. 235:783–804.

Henderson, R., J. M. Ritchie, and G. R. Strichartz. 1974. Evidence that tetrodotoxin and saxitoxin act at a metal cation binding site in the sodium channels of nerve membrane. *Proceedings of the National Academy of Sciences*. 71:3936–3940.

Hille, B. 1968. Pharmacological modifications of the sodium channels of frog nerve. *Journal of General Physiology*. 51:199–219.

Hille, B. 1971. The permeability of the sodium channel to organic cations in myelinated nerve. *Journal of General Physiology*. 58:599–619.

Hille, B. 1975. The receptor for tetrodotoxin and saxitoxin: a structural hypothesis. *Biophysical Journal*. 15:615–619.

Hille, B. 1984. Ionic Channels of Excitable Membranes. Sinauer Associates, Inc., Sunderland, MA. 272–302.

Hille, B., J. M. Ritchie, and G. R. Strichartz. 1975*a*. The effect of surface charge on the nerve membrane on the action of tetrodotoxin and saxitoxin in frog myelinated nerve. *Journal of Physiology*. 250:34P–35P. (Abstr.)

Hille, B., A. M. Woodhull, and B. I. Shapiro. 1975*b*. Negative surface charge near sodium channels of nerve: divalent ions, monovalent ions, and pH. *Philosophical Transactions of the Royal Society of London, Series B*. 270:301–318.

Honig, B. H., W. L. Hubbell, and R. F. Flewelling. 1986. Electrostatic interactions in membranes and proteins. *Annual Reviews of Biophysics and Biophysical Chemistry*. 15:163–193.

Kao, C. Y., and A. Nishiyama. 1965. Actions of saxitoxin on peripheral neuromuscular systems. *Journal of Physiology*. 180:50–66.

Kao, C. Y., and S. E. Walker. 1982. Active groups of saxitoxin and tetrodotoxin as deduced from actions of saxitoxin analogues on frog muscle and squid axon. *Journal of Physiology*. 323:619–637.

Kao, C. Y., and T. Yasumoto. 1985. Actions of 4-epitetrodotoxin and anhydrotetrodotoxin on the squid axon. *Toxicon*. 23:725–729.

Krueger, B. K., R. W. Ratzlaff, G. R. Strichartz, and M. P. Blaustein. 1979. Saxitoxin binding to synaptosomes, membranes, and solubilized binding sites from rat brain. *Journal of Membrane Biology*. 50:287–310.

Krueger, B. K., J. F. Worley, and R. J. French. 1983. Single sodium channels from rat brain incorporated into planar lipid bilayer membranes. *Nature*. 303:172–175.

McLaughlin, S. 1977. Electrostatic potentials at membrane-solution interfaces. *Current Topics in Membranes and Transport*. 9:71–144.

McLaughlin, A., W.-K. Eng, G. Vaio, T. Wilson, and S. McLaughlin. 1983. Dimethonium, a divalent cation that exerts only a screening effect on the electrostatic potential. *Journal of Membrane Biology*. 76:183–193.

McLaughlin, S. G. A., G. Szabo, and G. Eisenman. 1971. Divalent ions and surface potential of charged phospholipid membranes. *Journal of General Physiology*. 58:667–687.

Miller, J. A., W. S. Agnew, and S. R. Levinson. 1983. Principal glycopeptide of the tetrodotoxin/saxitoxin binding protein from *Electrophorus electricus*: isolation and partial chemical and physical characterization. *Biochemistry*. 22:462–470.

Miller, R. G. 1974. The jackknife: a review. *Biometrika*. 61:1–15.

Moczydlowski, E., S. S. Garber, and C. Miller. 1984*a*. Batrachotoxin-activated Na^+ channels in planar lipid bilayers. Competition of tetrodotoxin block by Na^+. *Journal of General Physiology*. 84:665–686.

Moczydlowski, E., S. Hall, S. S. Garber, G. S. Strichartz, and C. Miller. 1984*b*. Voltage-dependent block of muscle channels by guanidinium toxins. Effect of toxin charge. *Journal of General Physiology*. 84:687–704.

Moczydlowski, E., A. Uehara, and S. Hall. 1986. Blocking pharmacology of batrachotoxin-activated sodium channels. *In* Ion Channel Reconstitution. C. Miller, editor. Plenum Publishing Corp., New York. 405–428.

Mullins, L. J. 1973. The use of models of the cell membrane in determining the mechanism of drug action. *In* A Guide to Molecular Pharmacology. R. M. Featherstone, editor. Marcel Dekker, New York. 1–52.

Narahashi, T., J. W. Moore, and W. R. Scott. 1964. Tetrodotoxin blockage of sodium conductance increase in lobster giant axon. *Journal of General Physiology*. 47:965–974.

Neumcke, B., and R. Stämpfli. 1986. The influence of SCN modified surface charges on nodal Na channels of frog nerve. *Progress in Zoology*. In press.

Pethig, R. 1979. Dielectric and Electronic Properties of Biological Materials. John Wiley & Sons, New York. 63–66.

Quandt, F. N., J. Z. Yeh, and T. Narahashi. 1985. All or none block of single Na^+ channels by tetrodotoxin. *Neuroscience Letters*. 54:77–83.

Rando, T. A., and G. R. Strichartz. 1985. Voltage dependence of saxitoxin block of Na channels appears to be a property unique to batrachotoxin-modified channels. *Journal of General Physiology*. 86:14*a*. (Abstr.)

Rando, T. A., and G. R. Strichartz. 1986. Saxitoxin blocks batrachotoxin-modified sodium currents in the node of Ranvier in a voltage-dependent manner. *Biophysical Journal*. 49:785–794.

Reed, J., and M. Raftery. 1976. Properties of the tetrodotoxin binding component in plasma membranes isolated from *Electrophorus electricus*. *Biochemistry*. 15:944–953.

Rhoden, V. A., and S. M. Goldin. 1979. The binding of saxitoxin to axolemma of mammalian brain. *Journal of Biological Chemistry*. 254:11199–11201.

Ritchie, J. M., and R. B. Rogart. 1977. The binding of saxitoxin and tetrodotoxin to excitable tissue. *Reviews of Physiology, Biochemistry and Pharmacology*. 79:1–50.

Schwarz, J. R., W. Ulbricht, and H.-H. Wagner. 1973. The rate of action of tetrodotoxin on myelinated nerve fibers of *Xenopus laevis* and *Rana esculenta*. *Journal of Physiology*. 233:167–194.

Shimizu, Y., C. Hsu, and A. Genenah. 1981. Structure of saxitoxin in solutions and stereochemistry of dihydrosaxitoxins. *Journal of the American Chemical Society.* 103:605–609.

Shrager, P., and C. Profera. 1973. Inhibition of the receptor for tetrodotoxin in nerve membranes by reagents modifying carboxyl groups. *Biochimica et Biophysica Acta.* 318:141–146.

Sigworth, F. J., and B. C. Spalding. 1980. Chemical modification reduces the conductance of sodium channels in nerve. *Nature.* 283:293–295.

Spalding, B. C. 1980. Properties of toxin-resistant sodium channels produced by chemical modification in frog skeletal muscle. *Journal of Physiology.* 305:485–500.

Strichartz, G. 1984. Structural determinations of the affinity of saxitoxin for neuronal sodium channels. Electrophysiological studies on frog peripheral nerve. *Journal of General Physiology.* 84:281–305.

Ulbricht, W. and H.-H. Wagner. 1975*a*. The influence of pH on equilibrium effects of tetrodotoxin on myelinated nerve fibers of *Rana esculenta*. *Journal of Physiology.* 252:159–184.

Ulbricht, W., and H.-H. Wagner. 1975*b*. The influence of pH on the rate of tetrodotoxin action on myelinated nerve fibers. *Journal of Physiology.* 252:185–202.

Wagner, H.-H., and W. Ulbricht. 1975. The rates of saxitoxin action and of saxitoxin-tetrodotoxin interaction at the node of Ranvier. *Pflügers Archiv.* 359:297–315.

Weast, R. C. 1972. Handbook of Chemistry and Physics. The Chemical Rubber Co., Cleveland, OH.

Weigele, J. B., and R. L. Barchi. 1978. Saxitoxin binding to the mammalian sodium channel. Competition by monovalent and divalent cations. *FEBS Letters.* 95:49–53.

Winiski, A. P., A. C. McLaughlin, R. V. McDaniel, M. Eisenberg, and S. McLaughlin. 1986. An experimental test of the discreteness-of-charge effect in positive and negative lipid bilayers. *Biochemistry.* 25:8206–8214.

Woodhull, A. 1973. Ionic blockage of sodium channels in nerve. *Journal of General Physiology.* 84:361–377.

Woodward, A. M. 1964. The structure of tetrodotoxin. *Pure and Applied Chemistry.* 9:49–74.

Worley, J. F., III, R. J. French, and B. K. Krueger. 1986. Trimethyloxonium modification of single batrachotoxin-activated sodium channels in planar bilayers. Changes in unit conductance and in block by saxitoxin and calcium. *Journal of General Physiology.* 87:327–349.